Basketballs as spherical acoustic cavities

Daniel A. Russell[a]

Department of Physics, Kettering University, Flint, Michigan 48504

The sound field resulting from striking a basketball is found to be rich in frequency content, with over 50 partials in the frequency range of 0–12 kHz. The frequencies are found to closely match theoretical expectations for standing wave patterns inside a spherical cavity. Because of the degenerate nature of the mode shapes, explicit identification of the modes is not possible without internal investigation with a microphone probe. A basketball proves to be an interesting application of a boundary value problem involving spherical coordinates. © *2010 American Association of Physics Teachers.*
[DOI: 10.1119/1.3290176]

I. INTRODUCTION

When a basketball bounces, the resulting compression and relaxation after impact with the surface give rise to a "thump" sound that is short in duration and low frequency in spectral content.[1] However, if a basketball is held in one hand and struck by a metal rod, the predominant sound is a metallic sounding "ping" that rings for a second or more after the ball is struck. In this paper we explain this ringing sound as due to standing sound waves within the interior spherical cavity of the basketball.

Discussions of standing sound waves in a spherical cavity are found mostly in graduate level textbooks in mathematical physics[2] or acoustics,[3,4] and even then the details are sometimes left for homework problems.[5] Spherical or hemispherical rooms are rarely constructed, despite their aesthetic shape, because the acoustic conditions can be disastrous and require strategic application of absorbing materials to render the room useable.[6]

Spherical acoustic resonators are important because they are used to measure the speed of sound in gases with high precision[7–9] and currently provide the most accurate means of measuring the universal gas constant.[10] The analysis of a spherical cavity requires the use of Legendre polynomials and spherical Bessel functions and necessitates a computational approach to visualize the mode shapes.[11] Undergraduate and graduate students typically encounter these functions in quantum mechanics courses, especially if spherical quantum wells are discussed.[12] A discussion of sound waves inside a spherical cavity provides a useful and interesting complementary encounter with these functions and shapes.

II. ACOUSTIC RESPONSE OF A BASKETBALL

Figure 1 shows the frequency spectrum of the sound resulting from striking a fully inflated basketball with a metal rod. The basketball was supported with rubber bands and the acoustic response was recorded with a high quality audio microphone approximately 1 cm from the basketball's outer surface. The frequency spectrum was obtained using a Fourier analyzer over a range of 0–6.8 kHz with a frequency resolution of 1 Hz. An average of ten impacts was taken. The spectrum shows some low frequency signal strength below 100 Hz, corresponding to the thump, but the spectrum is dominated by a large number of very prominent higher frequency peaks, some of which are more than 40 dB above the noise floor. Additional peaks were observed to extend be-

yond 12 kHz. Similar spectra have been reported for the acoustic signature of a 67 cm diameter plastic ball exposed to white noise.[13]

The first prominent peaks in the spectrum of Fig. 1 are a series of broad peaks between 400 and 600 Hz. An experimental modal analysis of the basketball confirms that these peaks are due to the structural vibration of the basketball shell. A small 0.5 g accelerometer was attached to the ball, and a force hammer was used to impact the ball at several locations around its surface. A two-channel Fourier analyzer was used to record frequency response functions (the ratio of acceleration response to force input) at 23 points evenly spaced around the surface of the ball. Modal parameters (frequencies, mode shapes, and damping) were extracted from the frequency response functions. Figure 2 shows the experimentally obtained fundamental vibrational mode shape of the basketball at the measured frequency of 410 Hz. The two images in Fig. 2 represent extremes of motion separated in time by half a period. The fundamental mode of a spherical shell is not spherically symmetric; the polar diameter of the spherical shell alternately elongates and contracts, while the equator respectively and simultaneously contracts and expands.[14]

Experimental modal analysis also identified structural modes at 564 and 616 Hz, but the damping in the rubber material is so high that it was not possible to obtain clean mode shapes at these frequencies. Higher order structural modes would be important for modeling the deformation of the ball as it bounces from a rigid floor but do not seem to contribute significantly to the acoustic spectra in Fig. 1, which is the focus of this paper.

The tall narrow peaks above 900 Hz in Fig. 1 were suspected to be due to standing sound waves in the interior of the basketball cavity. A finite element model of a rigid-walled, air-filled spherical cavity of radius 11.6 cm and with a speed of sound of 343 m/s was found to have standing wave patterns at 970 and 1580 Hz. Peaks near these frequencies are observed in the sound spectrum in Fig. 1, indicating that these peaks represent the first two cavity resonances inside the basketball. These, and many of the higher frequency resonances, will be matched with theory later in this paper.

III. THEORY FOR A SPHERICAL ACOUSTIC CAVITY

To examine the nature of the sound field inside a spherical cavity, we start with the three-dimensional wave equation for acoustic sound pressure,
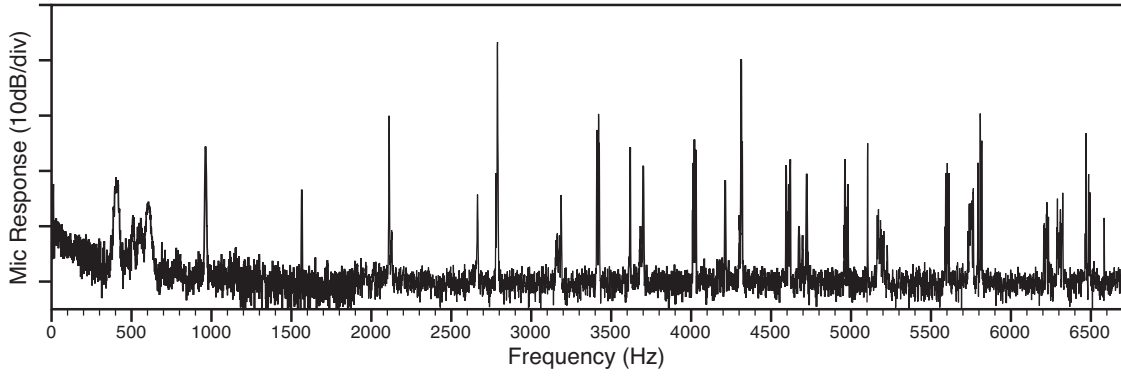
Fig. 1. Frequency spectrum of the microphone response due to striking a basketball with a metal rod. The spectrum represents the average of ten impacts.

$$\nabla^2 p - \frac{1}{c^2}\frac{\partial^2 p}{\partial t^2} = 0, \tag{1}$$

where c is the speed of sound. In spherical coordinates, the second-order spatial derivative $\nabla^2 p$ becomes

$$\nabla^2 p = \frac{1}{r^2}\frac{\partial}{\partial r}\left(r^2\frac{\partial p}{\partial r}\right) + \frac{1}{r^2\sin\theta}\frac{\partial}{\partial\theta}\left(\sin\theta\frac{\partial p}{\partial\theta}\right)$$

$$+ \frac{1}{r^2\sin^2\theta}\frac{\partial^2 p}{\partial\phi^2}. \tag{2}$$

For harmonic waves with the time dependence $e^{i\omega t}$, the wave equation may be written as

$$\frac{\partial}{\partial r}\left(r^2\frac{\partial p}{\partial r}\right) + \frac{1}{\sin\theta}\frac{\partial}{\partial\theta}\left(\sin\theta\frac{\partial p}{\partial\theta}\right) + \frac{1}{\sin^2\theta}\frac{\partial^2 p}{\partial\phi^2} + k^2 r^2 p$$

$$= 0, \tag{3}$$

where $k = \omega/c$, $\omega = 2\pi f$, and f is the frequency in hertz. It is tempting to interpret the quantity k as the familiar wavenumber $k = 2\pi/\lambda$ in terms of the wavelength λ. However, for waves in a three-dimensional bounded medium, k is actually the magnitude of a vector quantity whose components represent wave propagation in the radial and two angular directions. In such a case it is not possible to directionally resolve wavelengths. Instead we must deal only with the components of the wave vector.

The wave equation (3) may be solved using the method of separation of variables by assuming
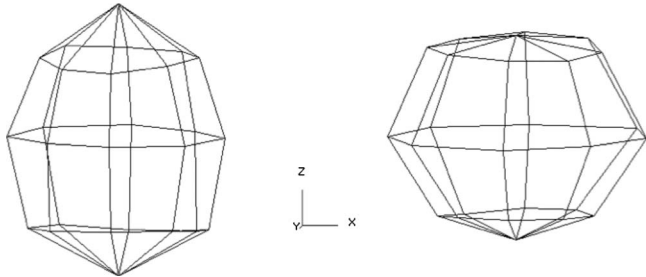

Fig. 2. Extremes of motion (separated in time by half a period) for the 410 Hz fundamental structural vibration mode of a basketball. The polar diameter elongates and contracts, while the equator contracts and expands.

$$p(r,\theta,\phi) = R(r)\Theta(\theta)\Phi(\phi). \tag{4}$$

We substitute this form into Eq. (3), carry out all the derivatives, and rearrange the terms to find the separable equations[4,12]

$$\frac{d^2\Phi}{d\phi^2} + m^2\Phi = 0, \tag{5}$$

$$\frac{1}{\sin\theta}\frac{d}{d\theta}\left(\sin\theta\frac{d\Theta}{d\theta}\right) + \left(\eta^2 - \frac{m^2}{\sin^2\theta}\right)\Theta = 0, \tag{6}$$

$$\frac{1}{r^2}\frac{d}{dr}\left(r^2\frac{dR}{dr}\right) + \left(k^2 - \frac{\eta^2}{r^2}\right)R = 0, \tag{7}$$

where m and η are the constants of separation.

Equation (5) governs the longitudinal spatial dependence on ϕ. Its solutions are

$$\Phi(\phi) = A\cos m\phi + B\sin m\phi, \tag{8}$$

where m must be an integer so that $\Phi(\phi)$ is single valued. There are no other restrictions on m so that this solution is really a pair of orthogonal degenerate solutions and may be written as

$$\Phi(\phi) = A\cos(m\phi + \gamma), \tag{9}$$

where A and γ depend on the initial conditions.

The latitudinal spatial dependence on θ is determined by Eq. (6). If $\eta^2 = \ell(\ell+1)$, then

$$\frac{1}{\sin\theta}\frac{d}{d\theta}\left(\sin\theta\frac{d\Theta}{d\theta}\right) + \left(\ell(\ell+1) - \frac{m^2}{\sin^2\theta}\right)\Theta = 0. \tag{10}$$

Its solutions are the associated Legendre polynomials of order m and degree ℓ,

$$\Theta(\theta) = P_\ell^m(\cos\theta), \tag{11}$$

where the order m and degree ℓ of the polynomial are related by $-\ell \le m < \ell$.

Equation (7) describes the spatial dependence of the sound field on the radial distance r from the center of the cavity. If we substitute $\eta^2 = \ell(\ell+1)$ and expand the derivative, Eq. (7) may be written as

$$\frac{d^2R}{dr^2} + \frac{2}{r}\frac{dR}{dr} + \left(k^2 - \frac{\ell(\ell+1)}{r^2}\right)R = 0, \qquad (12)$$

which is the spherical Bessel equation with solutions

$$R(r) = j_\ell(kr) + y_\ell(kr). \qquad (13)$$

$j_\ell(kr)$ and $y_\ell(kr)$ are, respectively, spherical Bessel functions of the first and second kind. $y_\ell(kr)$ become infinite at the origin, so they do not play a role in the sound field inside a hollow sphere. The spherical Bessel functions are related to the usual Bessel functions

$$j_\ell(kr) = \sqrt{\frac{\pi}{2r}} J_{\ell+(1/2)}(kr) \qquad (14)$$

and may also be expressed in terms of sine and cosine functions.[4,12]

IV. RESONANCE FREQUENCIES AND MODE SHAPES

The boundary conditions for sound waves in a spherical cavity require that the sound pressure be finite at the center and that the particle displacement and velocity be zero for $r=a$ at the cavity surface. The sound pressure p and particle velocity u in a sound wave are related through conservation of momentum by Euler's equation,[15]

$$\rho\frac{\partial u}{\partial t} = -\frac{\partial p}{\partial r}, \qquad (15)$$

where ρ is the density of the gas in the cavity. The boundary condition of zero velocity at the surface means that the resonance frequencies of the spherical cavity may be determined from the values of k that satisfy

$$\frac{\partial}{\partial r}j_\ell(kr)\big|_{r=a} = 0. \qquad (16)$$

The values of k satisfying this boundary condition are

$$k_{n\ell} = z_{n\ell}/a, \qquad (17)$$

where $z_{n\ell}$ is the nth zero of the derivative of the spherical Bessel function of order ℓ. The resulting resonance frequencies,

$$f_{n\ell} = \frac{z_{n\ell}c}{2\pi a}, \qquad (18)$$

do not depend on the index m because of the degeneracy with ϕ.

The mode shapes corresponding to standing waves inside a spherical cavity are due to contributions from Eqs. (8), (11), and (13), which we combine as

$$p_{n\ell m} = A_{n\ell m}j_\ell(k_{n\ell}r)P_\ell^m(\cos\theta)\cos(m\phi + \gamma_{n\ell m}), \qquad (19)$$

where $A_{n\ell m}$ and $\gamma_{n\ell m}$ depend on initial conditions.

We identify mode shapes using the notation (n,ℓ,m) according to the number of nodal surfaces in the (r,θ,ϕ) directions. Acoustic modes for which $m=0$, such as $(1,1,0)$, $(1,2,0)$, $(1,3,0)$ and $(2,0,0)$, are called *zonal* harmonics. These mode shapes are independent of ϕ and are symmetric about the z-axis. Acoustic modes for which $m=\ell$, such as $(1,1,1)$, $(1,2,2)$, and $(1,3,3)$, are *sectoral* harmonics and have no nodes in the latitudinal or θ direction. All other modes are

Table I. Theoretical and measured frequencies (in hertz) for the first 24 resonances of a spherical cavity of inner radius 0.116 m. Measured frequencies have an uncertainty of ± 1 Hz. The frequency ranges indicate separation of degenerate modes due to irregularities in the basketball interior.

Measured frequency	Probable mode shape (n,ℓ,m)	Theoretical frequency
963	$(1,1,m)$	979
1565	$(1,2,m)$	1572
2111	$(2,0,0)$	2113
2129	$(1,3,m)$	2122
2664	$(1,4,m)$	2659
2780–2789	$(2,1,m)$	2795
3154–3187	$(1,5,m)$	3181
3412–3426	$(2,2,m)$	3431
3619	$(3,0,0)$	3638
3684–3701	$(1,6,m)$	3694
4010–4028	$(2,3,m)$	4038
4213	$(1,7,m)$	4203
4313–4319	$(3,1,m)$	4334
4594–4620	$(2,4,m)$	4631
4674–4723	$(1,8,m)$	4711
4962–4980	$(3,2,m)$	4993
5104	$(4,0,0)$	5130
5164–5205	$(2,5,m)$	5210
5226	$(1,9,m)$	5214
5588–5613	$(3,3,m)$	5633
5731–5765	$(2,6,m)$	5779
5794–5818	$(4,1,m)$	5836
6209–6235	$(3,4,m)$	6259
6291–6324	$(2,7,m)$	6339

tesseral harmonics.

From Eqs. (17) and (18) we find that the lowest frequency corresponds to the degenerate pair of modes $(1,1,m)$ for which $k_{11}a=2.08$, resulting in a frequency of 979 Hz for an air-filled cavity of radius 11.6 cm. The next frequency corresponds to the degenerate modes $(1,2,m)$, with $k_{12}a=3.34$ and a calculated frequency of 1572 Hz.

For spherically symmetric radial modes with $\ell=m=0$, the spherical Bessel function is

$$j_0(kr) = \frac{\sin(kr)}{kr}, \qquad (20)$$

and the boundary condition in Eq. (16) becomes

$$\tan k_{n0}a = k_{n0}a, \qquad (21)$$

with roots $k_{n0}a = 0, 4.49, 7.73, 10.90, 14.07, \ldots$. Thus the $(2,0,0)$ radial mode for an air-filled spherical cavity of radius 11.6 cm has a frequency of 2113 Hz. Rayleigh predicted frequency ratios[3] for these symmetric vibrations as $f_{300}/f_{200}=1.719$ and $f_{400}/f_{200}=2.427$. Rayleigh also predicted that the lowest resonance frequency of the spherical cavity, the $(1,1,m)$ mode, would be more than an octave lower than that of the first spherically symmetric mode $(2,0,0)$. Both predictions are consistent with the data in Table I.

Figures 3 and 4 illustrate two methods of visualizing the lowest order mode shapes in a spherical cavity. In Fig. 3 the modes are identified by drawing nodal surfaces on which the sound pressure is zero.[4] As the latitudinal direction is tra-

(1,1,0) **(1,1,1)**
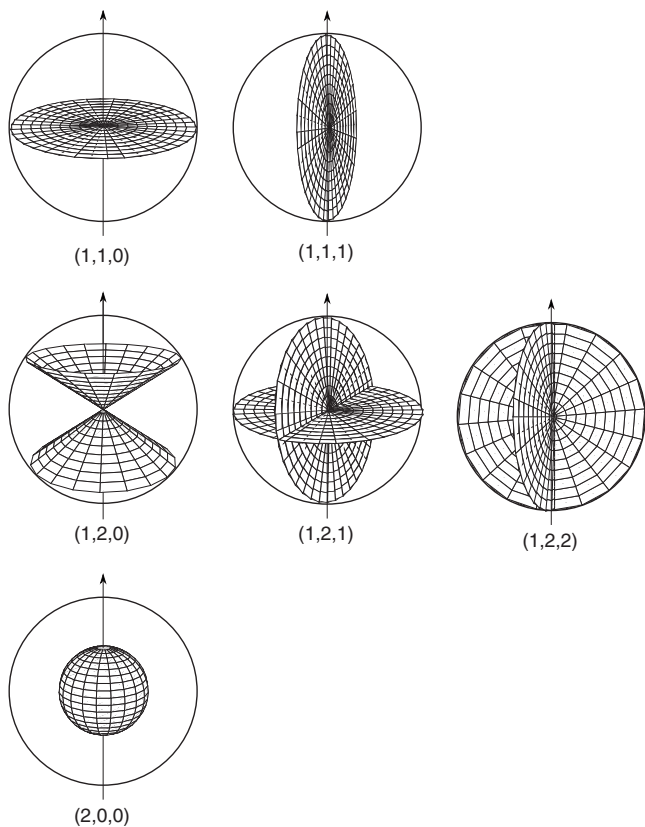
(1,2,0) **(1,2,1)** **(1,2,2)**

(2,0,0)

Fig. 3. Pressure nodal surfaces for the lowest nonradial modes and the first radial mode of a spherical cavity. Modes are designated by indices (n,ℓ,m), and modes in each row are degenerate modes with identical frequencies (after Ref. 4).

(1,1,0) **(1,1,1)**

(1,2,0) **(1,2,1)** **(1,2,2)**
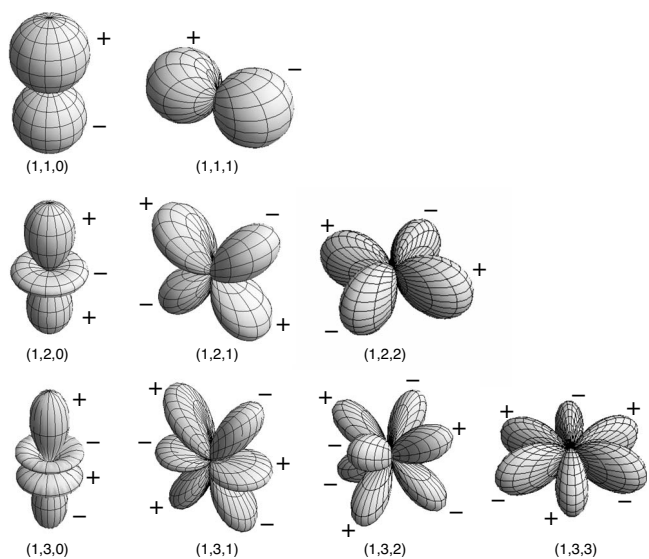
(1,3,0) **(1,3,1)** **(1,3,2)** **(1,3,3)**

Fig. 4. Nonradial mode shapes representing the sound pressure amplitude at a constant distance from the center of the sphere for several lowest modes (n,ℓ,m) of a spherical cavity, corresponding to some of the nodal surface maps in Fig. 3. Adjacent lobes have opposite phase, as indicated by + and − signs. Modes in each row with the same value of ℓ are degenerate modes with identical frequencies.

versed from the top to the bottom over the surface of the spherical cavity, $(\ell-m)$ nodal surfaces are encountered, whereas traversing the surface of the sphere in the longitudinal direction yields $2m$ nodal surfaces. The $\ell=1$ and $\ell=2$ families of mode shapes are nonradial modes for which the air in the cavity oscillates back and forth from side to side or moves in a tangential direction around the circumference. For the $(1,1,0)$ mode, the (x,y) plane (corresponding to $\theta=\pi/2$) is a nodal surface, and for the $(1,1,1)$ mode, any meridian plane is a nodal surface. The nodal surface for the $(1,2,0)$ mode is a cone with its vertex at the center of the sphere. The $(2,0,0)$ mode is the first radial mode, and its nodal surface is a sphere with radius $r=0.582a$.

An alternate method of visualizing mode shapes shown in Fig. 4 visualizes the mode shapes using surfaces that represent the amplitude of the sound pressure as a function of angular direction at a fixed radial distance from the center of the spherical cavity. Adjacent lobes have opposite phases as indicated by the + and − signs. The mode shapes in Fig. 4 look similar to the shapes representing probability distributions $|\Psi|^2$ for the first few hydrogen wave functions.[12] This similarity is not surprising because the same mathematics is responsible for both phenomena. It is also possible to visualize mode shape cross-sections using density plots.[11,12]

It is worth spending some time to understand what the shapes in Figs. 3 and 4 represent. For the $(1,1,0)$ mode, the pressure nodal surface comprising the equatorial plane in Fig. 3 represents locations where the pressure is zero. The sound pressure amplitude is maximum near the north and

south poles of the sphere, with opposite phases as indicated in the $(1,1,0)$ mode shape in Fig. 4. In this mode shape, the air in the cavity oscillates back and forth between the upper and lower hemispheres, following a path with radial and tangential components. The velocity and displacement of the air particles are maximum at the equatorial plane. The behavior of the $(1,1,1)$ mode is similar, with air oscillating back and forth between the left and right hemispheres.

For the $(1,2,0)$ mode the surfaces of zero sound pressure are cones with vertices at the center of the sphere (see Fig. 3). If we assume that the sound pressure amplitude starts out positive at the north and south poles and negative around the equator, as indicated in Fig. 4, the air molecules oscillate along paths tangent to the spherical surface (with no radial components of motion) from both poles simultaneously toward the equator and then back toward the poles. For the $(1,2,1)$ mode the surfaces of zero sound pressure are planes and divide the sphere into quadrants. As the mode oscillates, air in each quadrant moves in and out of the adjacent quadrants. For example, some of the air molecules in the upper right quadrant move, in a mostly tangential direction, clockwise toward the lower right quadrant, while other air molecules move counterclockwise toward the upper left quadrant. The particle displacement and velocity are maximum at the locations of the nodal surfaces in Fig. 3. Conversely, the particle displacement and velocity are zero where the sound pressure amplitude is maximum, corresponding to the lobes of the pressure amplitude shapes shown in Fig. 4. The behavior of the $(1,2,2)$ mode is similar.

For the radially symmetric $(2,0,0)$ mode, the sound pressure nodal surface is a sphere, and the air particle motion is purely radial. Air molecules oscillate along radial paths away from the center toward the surface $r=a$ and back toward the center. The sound pressure amplitude at the center of the sphere is greater than the amplitude at the surface $r=a$ because of the nature of the radial dependence of the Bessel function.

Modes for which m and ℓ are both less than n involve waves that reflect perpendicularly from the spherical surface of the cavity and focus strongly at the center of the sphere.[2,6] For modes where m and ℓ are both much greater than n, the waves tend to travel in paths tangent to the sphere surface and thus avoid the center of the sphere. The pressure amplitude for these modes is small throughout most of the cavity and large only near the cavity walls.

V. MATCHING MEASUREMENT TO THEORY

The National Collegiate Athletic Association[16] requires a properly inflated basketball to have an outer circumference between 29.5 and 30 in. (749–762 mm),[17] corresponding to an outer radius of 12.0 cm. If we assume a wall thickness of 0.4 cm, we find a radius of $a = 11.6$ cm for our spherical cavity, in agreement with Refs. 1, 18, and 19. The speed of sound inside the basketball was taken to be $c = 343$ m/s. Table I compares the theoretical frequencies calculated from Eq. (18) to the measured frequency values. Several measured frequencies, including the $(1,1,m)$ and $(1,2,m)$ modes, are slightly lower than the theoretical values, and other measured frequencies for higher modes are higher than theory. These discrepancies could be due to coupling between the shell and internal acoustic modes[20] but more likely result from the interior of the basketball not being perfectly spherical.

A detailed inspection of the frequency spectrum reveals some interesting observations. Theory predicts that the $(2,0,0)$ and $(1,3,m)$ modes are separated by only 9 Hz, with frequencies of 2113 and 2122 Hz, respectively. The spectrum in Fig. 1 appears to show a single strong peak near 2100 Hz,

but a closer look at the spectrum, as shown in Fig. 5, reveals a strong peak at 2111 Hz and a smaller but distinct peak at 2129 Hz. The purely radial modes $(n,0,0)$ show up in Fig. 5 as narrow single peaks. Modes with $n = 1$ also show up as narrow single peaks. However, the magnified view of the spectrum shows that most of the other degenerate modes exhibit multiple peaks, indicating that the degenerate shapes that should occur at the same frequency are split among several closely spaced frequencies. This mode splitting is most likely due to the basketball interior not being a perfect sphere.

Even with the observed mode splitting that separates the degeneracies, an external measurement of the interior sound field with a single microphone cannot distinguish which mode or modes are present at those frequencies. It is possible to identify some of the lowest order degenerate modes by using two microphones at different locations and comparing signal strengths.[21] The differences between the measured and theoretical frequencies for radially symmetric modes and the frequency splits between degenerate modes can be used to determine the extent to which the exact shape of the spherical cavity deviates from a perfect sphere.[22,23] However, the precision of the measurements of frequencies and resonator volumes required to make such estimates is far beyond those used in the present analysis.

VI. CONCLUSIONS AND FURTHER EXPLORATION

We have shown that the sound resulting from striking a fully inflated basketball may be explained by modeling the interior of the ball as a spherical acoustic cavity. Resonances in the measured frequency spectrum are consistent with predicted frequencies.

A challenging undergraduate project would be to drive and map the first several standing waves inside a spherical cavity. One could obtain or construct a large transparent plastic spherical shell. Transparency would facilitate interrogation of the interior. Small loudspeakers could be used to drive specific modes and a small microphone could be used to measure the standing wave patterns. Locations of nodal surfaces could be determined by observing the Lissajous pattern between input and output signals,[24] or one could adapt the approach recently used to identify resonances in a cylindrical acoustic resonator.[25] The excess of degenerate modes and the potential for mode mixing would preclude the identification of each of the individual modes for each frequency in Table I. But the identification and mapping of the mode shapes shown in Fig. 3 should be possible.

Fig. 5. Details of the frequency spectrum from Fig. 1 showing the frequency splitting of degenerate modes.

a)Electronic mail: drussell@kettering.edu
[1] J. I. Katz, "Thump, ring: The sound of a bouncing ball," arXiv:0808.3278.
[2] P. M. Morse and H. Feshbach, *Methods of Theoretical Physics* (McGraw-Hill, New York, 1953), pp. 1468–1472.
[3] J. W. S. Rayleigh, *Theory of Sound*, 2nd ed. (Dover, New York, 1945), Vol. 2, pp. 264–268.
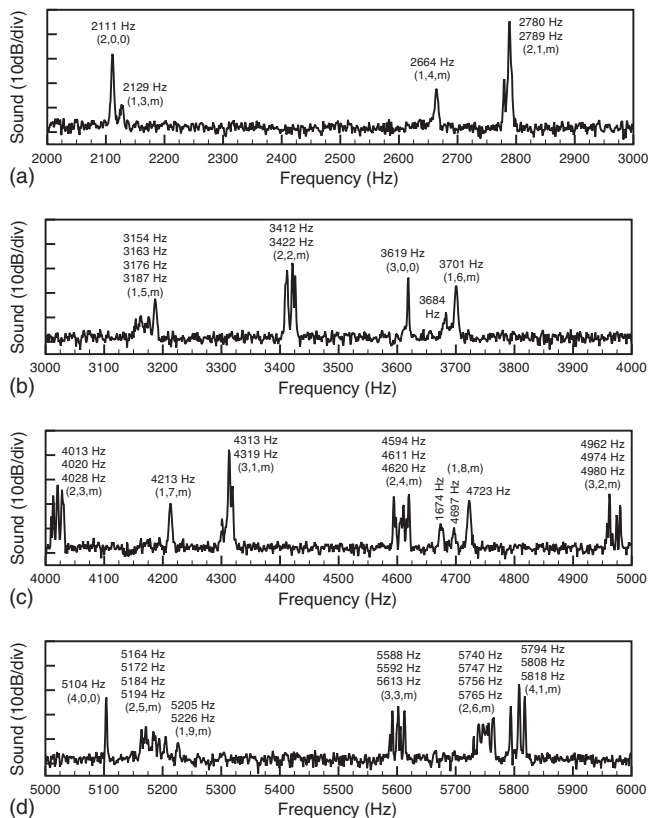
[4] L. E. Kinsler, A. R. Frey, A. B. Coppens, and J. V. Sanders, *Fundamentals of Acoustics*, 4th ed. (Wiley, New York, 2000), pp. 250–252, 513–514.

[5] D. T. Blackstock, *Fundamentals of Physical Acoustics* (Wiley, New York, 2000), pp. 335–356.

[6] J. L. Flanagan, "Acoustic modes of a hemispherical room," J. Acoust. Soc. Am. **37** (4), 616–618 (1965).

[7] D. Bancroft, "Measurement of velocity of sound in gases," Am. J. Phys. **24** (5), 355–358 (1956).

[8] M. R. Moldover, J. B. Mehl, and M. Greenspan, "Gas-filled spherical resonators: Theory and experiment," J. Acoust. Soc. Am. **79** (2), 253–272 (1986).

[9] G. Bendetto, R. M. Gavioso, and R. Spagnolo, "Precision measurement of speed of sound in gases," in *Proceedings of the 16th IEEE Instrumentation and Measurement Technology Conference*, Venice, Italy, 24–26 May 1999 (IEEE, 1999), pp. 1837–1841.

[10] M. R. Moldover, J. P. M. Trusler, T. J. Edwards, J. B. Mehl, and R. S. Davis, "Measurement of the universal gas constant R using a spherical acoustic resonator," Phys. Rev. Lett. **60** (4), 249–252 (1988).

[11] S. P. Lipshitz, R. Portugal, and J. Vanderkooy, "Using computer algebra to explore sound-wave propagation in spherical cavities," Comput. Sci. Eng. **2** (2), 85–94 (2000).

[12] D. J. Griffiths, *Introduction to Quantum Mechanics*, 2nd ed. (Pearson-Prentice-Hall, Upper Saddle River, NJ, 2005), pp. 131–157.

[13] D. Rocchesso and P. Dutilleux, "Generalization of a 3-D acoustic resonator model for the simulation of spherical enclosures," EURASIP J. Appl. Signal Process. **2001** (1), 15–26 (2001).

[14] H. Lamb, "On the vibrations of a spherical shell," Proc. London Math. Soc. **S1–14**, 50–56 (1882).

[15] Reference 3, pp. 117–119.

[16] *2009 NCAA Men's and Women's Basketball Rules*, edited by L. Danehy (National Collegiate Athletics Association, Indianapolis, IN, 2008), pp. 36–37.

[17] The regulation states that a properly inflated ball, when dropped from a height of 6 ft (measured from the bottom of the ball), will rebound from the playing surface to a height of no more than 54 in. and no less than 49 in. (measured from the top of the ball).

[18] P. J. Brancazio and H. Brody, "How much air is in a basketball?," Am. J. Phys. **55** (3), 276 (1987).

[19] H. Brody, "An experiment to measure the density of air," Phys. Teach. **27** (1), 46 (1989).

[20] J. B. Mehl, "Spherical acoustic resonator: Effects of shell motion," J. Acoust. Soc. Am. **78** (2), 782–788 (1985).

[21] A. Karbach and P. Hess, "Laser excitation of acoustic resonances in a spherical resonator," J. Appl. Phys. **58** (10), 3851–3855 (1985).

[22] J. B. Mehl, "Acoustic resonance frequencies of deformed spherical resonators," J. Acoust. Soc. Am. **71** (5), 1109–1113 (1982).

[23] J. B. Mehl, "Acoustic resonance frequencies of deformed spherical resonators. II," J. Acoust. Soc. Am. **79** (2), 278–285 (1986).

[24] T. D. Rossing and D. A. Russell, "Laboratory observation of elastic waves in solids," Am. J. Phys. **58** (12), 1153–1162 (1990).

[25] M. J. Moloney, "Plastic CD containers as cylindrical acoustical resonators," Am. J. Phys. **77** (10), 882–885 (2009).

Regulatory Mechanisms in Complex Systems

Why did nature make life so complex? Much of the complexity seems overdone. Our bodies are constantly at work to hold variables within narrow limits. This internal regulatory function is called homeostasis. We expect our body temperature, pulse rate, and blood pressure to be reasonably constant. All complex systems have regulatory mechanisms that constrain variables. Societies are homeostatic. They have religions, custom, black magic, laws, and countless prescribed behavioral patterns that produce order out of what otherwise becomes chaotic and self-destructive. Ecologies evolve to quasi-equilibrium and incorporate homeostatic constraints. Much of our complexity seems to be on standby, to be called on when adjustments to changing environments are needed.

George A. Cowan, *Manhattan Project to the Santa Fe Institute* (University of New Mexico Press, 2010) pp. 130-131.